Neoplasma 2023; 70(2): 229–239

doi:10.4149/neo_2023_220828N871

High expression of WTAP is related to poor prognosis in nasopharyngeal carcinoma

Chang-Juan TAO[1,2,#], Peng ZHANG[3,#], Yuan-Yuan CHEN[4], Ming CHEN[1,*]

[1]Department of Radiation Oncology, The Second Affiliate Hospital of Soochow University, Suzhou, Jiangsu, China; [2]Department of Radiation Oncology, Zhejiang Cancer Hospital, Institute of Basic Medicine and Cancer (IBMC), Chinese Academy of Sciences, Hangzhou, Zhejiang, China; [3]Department of Medical Oncology, Zhejiang Cancer Hospital, Institute of Basic Medicine and Cancer (IBMC), Chinese Academy of Sciences, Hangzhou, Zhejiang, China; [4]Department of Radiation Oncology, Sun Yat-Sen University Cancer Center, State Key Laboratory of Oncology in South China, Collaborative Innovation Center for Cancer Medicine, Guangzhou, Guangdong, China

**Correspondence: chenming@sysucc.org.cn*
[#]Contributed equally to this work.

Received August 28, 2022 / Accepted March 9, 2023

Wilms' tumor 1-associated protein (WTAP), a component of the m6A methyltransferase complex, recruits the m6A methyltransferases METTL3 and METTL14 to the corresponding mRNA targets to participate in the formation of N6-methyladenosine. However, the molecular mechanism of WTAP in the tumorigenesis and progression of nasopharyngeal carcinoma (NPC) remains unclear. This study aimed to explore the prognostic value and biological function of WTAP in NPC. We assessed WTAP expression and its prognostic significance using microarray datasets from the Gene Expression Omnibus (GSE12452) database and 100 NPC tissues via bioinformatics analysis and immunohistochemistry (IHC), respectively. Moreover, gene ontology (GO) and gene set enrichment analysis (GSEA) were performed. In addition, the correlation of WTAP expression with the expression of immune cell biomarkers was analyzed. The results showed that WTAP expression was significantly overexpressed in NPC tissues in GSE12452. The overexpression of WTAP was validated by the external datasets including NPC tissues (GSE150430) and NPC cell lines (GSE39826). GO analysis suggested enrichment in the nucleoplasm (cellular component) and cell cycle (biological process). The GSEA revealed that differentially expressed genes were enriched in E2F-targets, Myc_targets_v1, G2M checkpoint, Myc_targets_v2, and Interferon-alpha-response. In IHC analysis, WTAP was upregulated in NPC tissues, and high levels of WTAP expression were significantly correlated with the advanced T stage (p=0.047) and advanced N stage (p=0.018). Cox regression demonstrated that WTAP overexpression was an independent biomarker of poor prognosis for overall survival (hazard ratio [HR], 4.747; 95% confidence interval [CI], 1.671–13.482; p=0.003). In IHC analysis, the expression of WTAP was positively correlated with CD206 (biomarker for M2 macrophages) (p=0.018) but negatively correlated with CD8a (biomarker for cytotoxic T cells) (p=0.001). In conclusion, WTAP is a promising prognostic biomarker and may participate in the regulation of immune cell infiltration in NPC.

Key words: WTAP; nasopharyngeal carcinoma; m6A methylation; survival; immune cell infiltration

Nasopharyngeal carcinoma (NPC) is a common type of malignancy in south China, southeastern Asia, and North Africa, with an estimated 130,000 patients worldwide in 2018 [1]. The widespread application of intensity-modulated radiotherapy (IMRT) and comprehensive medical treatment (chemotherapy, targeted therapy, and immunotherapy) have improved the 5-year overall survival (OS) rates for patients with NPC to approximately 85% [2]. However, substantial inter-individual prognostic differences were observed in patients with NPC with the same tumor-node-metastasis (TNM) stage. Emerging evidence suggests that the TNM stage only represents the invasion of anatomical structure but does not indicate the inherent biological characteristics of the tumor. Many novel biomarkers, including Epstein-Barr virus (EBV)-DNA copy number [3], proteomics [4], micro-RNA [5], immune score [6], and radiomics [7], were validated to complement the TNM staging system and improve the predictive and prognostic value.

N6-methyladenosine (m6A) is the most abundant RNA modification in eukaryotic cells, which plays a vital role in various aspects of RNA metabolism, including pre-mRNA splicing, 3'-end processing, nuclear export, translation regulation, mRNA decay, and noncoding RNA (ncRNA) processing [8]. m6A methylation is accomplished through the dynamic regulation of "writers", "erasers", and "readers", which are proteins that can add, remove, or recognize

m6A-modified sites. m6A methylation is catalyzed by an important methyltransferase complex comprising methyltransferase-like 3 (METTL3), METTL14, and Wilms' tumor 1-associated protein (WTAP).

Increasing evidence suggests that m6A RNA methylation plays an important role as an oncogene or suppressor in the occurrence and progression of various tumors. WTAP is a highly conserved nuclear protein, a binding partner of WT1 first identified by Little et al. [9]. It has been reported that WTAP is associated with the malignant progression of cancers. High expression of WTAP has been verified to be a biomarker of poor prognosis in pancreatic ductal adenocarcinoma [10], bladder cancer [11], gastric cancer [12], acute myeloid leukemia [13], and glioblastoma [14]. Additionally, Chen et al. systematically elucidated the oncogene function of WTAP in nasopharyngeal carcinoma; the results found that WTAP-mediated m6A modification of lncRNA DIAPH1-AS1 enhances its stability to facilitate nasopharyngeal carcinoma growth and metastasis [15]. However, to the best of our knowledge, the relationship between WTAP and the immune microenvironment in nasopharyngeal carcinoma has not been investigated.

In the present study, we investigated the WTAP expression in NPC tissues and normal tissues in a public NPC database (GSE12452) and analyzed its prognostic significance in clinical biopsy samples. Furthermore, we performed an exploratory analysis of the correlation between WTAP expression and immune cell infiltration in NPC.

Patients and methods

Data mining from public databases. Gene Expression Omnibus (GEO) (https://www.ncbi.nlm.nih.gov/geo/), which collects submitted high throughput gene expression data, was queried thoroughly for all datasets involving NPC. The inclusion criteria for the datasets were as follows: 1) *Homo sapiens* as the organism; 2) samples containing NPC tissues (n>5) and normal nasopharyngeal tissues (n>5); 3) expression profiling by the array as the study type; 4) datasets as the entry type; 5) total RNA samples for transcriptome testing; 6) studies with clinical sample characteristics. Additionally, samples from patients who received preoperative treatment were excluded. Based on these criteria, GSE12452 was selected. Then the raw data and corresponding clinical information were downloaded from GEO for further analysis. The array dataset (GSE12452) consisted of 10 normal nasopharyngeal tissue samples and 31 NPC samples. The expression of WTAP was validated by the external datasets that included NPC tissues (GSE150430) and NPC cell lines (GSE39826) [16, 17]. Gene expression profiles of the NPC and non-cancerous tissues were assessed using the Human Genome U133 Plus 2.0 Array (Affymetrix, Santa Clara, CA, USA), and expression levels were calculated using Nexus Expression 3 software (BioDiscovery, El Segundo, CA, USA). The probe expression file was imported, and all genes were analyzed according to the probe set annotation file. Functional candidate genes were identified by comparing the gene transcription levels between tumor and non-tumor tissues using the limma package in R software (3.6.1 version). Genes with significantly different expression levels were further analyzed ($\log_2$ FC>1 or $\log_2$ FC<–1; $p<0.05$). The functional role of WTAP in NPC (vs. normal sample) was further explored by Gene Ontology (GO) and gene set enrichment analysis (GSEA). The GO was analyzed using the DAVID database (https://david.ncifcrf.gov/) and GSEA was performed with the clusterProfiler R/Bioconductor package. GSEA generated an ordered list of all genes according to WTAP expression using the GSEA hallmark gene set [18]. The GO and GSEA were also performed in the high-WTAP and the low-WTAP expression groups to explore the biological signaling pathway. Furthermore, we assessed whether WTAP expression is correlated with the expression of specific markers of T cells, B cells, M1 cells, M2 cells, Th1 cells, Th2 cells, and Treg cells in NPC.

Patients and specimens. Between January and June 2016, formalin-fixed, paraffin-embedded NPC tissue samples from 100 patients who underwent definitive chemoradiotherapy at Zhejiang Cancer Hospital, with complete clinicopathological information and follow-up data, were obtained and used to verify the prognostic value of WTAP in NPC. No patients received clinical treatment before sampling. The study protocol was approved by the ethics committee of the Zhejiang Cancer Hospital (NO: IRB-2020-3). Written consent was waived because this was a retrospective study; verbal consent was obtained from the patients via telephone and documented in the informed consent form if the patient agreed to participate in this study. The Institutional Review Board approved the use of verbal consent.

Treatment methods. All patients were immobilized in the supine position with a head, neck, and shoulder thermoplastic mask. Two sets of images (i.e., with and without contrast) were obtained from the computed tomography (CT) simulator for treatment planning. The CT was performed after intravenous contrast medium administration, and 3 mm slices from the head to 1 cm below the sternoclavicular joint were obtained. The target volumes were delineated according to the recommendations of the International Commission on Radiation Units and Measurements reports 50 and 62. The clinical target volumes (CTVs) were individually delineated based on the tumor invasion pattern, as described previously [19]. The contoured images were transferred to an inverse IMRT planning system (Pinnacle version 7.6, Philips Medical Systems, Bothell, WA, USA). The prescribed radiation dose (i.e., the minimum dose received by 95% of the planning target volume [PTV]) was a total dose of 69–69.9 Gy in 30–33 fractions to the PTV of the primary gross tumor volume (GTV), 67.5–69.9 Gy to the nodal GTV PTV, 60 Gy to the CTV-1 PTV (i.e., high-risk regions), and 54 Gy to the CTV-2 PTV (i.e., low-risk regions) and CTV-N (i.e., neck nodal regions). All patients were treated with one

fraction daily for 5 days per week. All targets were treated simultaneously using the simultaneous integrated boost technique.

Overall, 5 patients (5%) were treated with radiotherapy alone and 95 patients (95%) received concurrent chemoradiotherapy. Ninety-three patients (93%) received neoadjuvant chemotherapy and 18 patients (18%) received adjuvant chemotherapy. Neoadjuvant or adjuvant chemotherapy consisted of cisplatin with 5-fluorouracil or taxanes every 3 weeks for two or three cycles. Concurrent chemotherapy consisted of cisplatin (80 mg/m^2 intravenously in three daily doses) and was given every 3 weeks for two cycles.

Immunohistochemistry of WTAP. The paraffin-embedded tissues were sectioned (4 μm), mounted on glass slides (MS-coated glass, Mats-unami, Osaka, Japan), and dried overnight at 37 °C. After deparaffinization, antigen retrieval was performed in 0.01 M citrate acid buffer, and inactivation of endogenous peroxidase activity was performed in 3% H_2O_2 in methanol for 10 min. Nonspecific binding was blocked by incubating the slides with 10% normal goat serum in phosphate-buffered saline for 1 h at room temperature. The slides were incubated with 1:1000 diluted anti-WTAP antibody (cat. no. ab195380; Abcam, Cambridge, UK) overnight at 4 °C. The IHC of immune cell biomarkers was performed as aforementioned. The following antibodies were used for IHC: CD8a antibody (cat. no. ab237710; Abcam, Cambridge, UK), CD206 antibody (cat. no. ab252921; Abcam, Cambridge, UK), CD68 antibody (cat. no. ab125212; Abcam, Cambridge, UK), CD200 antibody (cat. no. ab254193; Abcam, Cambridge, UK), Foxp3 (cat. no. ab243890; Abcam, Cambridge, UK) and PD-L1 (cat. no. ab205921; Abcam, Cambridge, UK). CD8a was stained as a marker of cytotoxic T cells and Foxp3 was a biomarker of Treg cells. CD68 was stained as a pan-macrophage marker, including M1 and M2 macrophages, while CD206 was stained as a biomarker for M2 macrophages [20]. The immunoreactivity was visualized using a streptavidin-biotin peroxidase staining kit (Histofine Simple Stain Max PO Multi, Nichirei, Tokyo, Japan) and DAB solution (Simple Stain DAB, Nichirei). Positive immunoreactivity was confirmed by the development of a brown chromogen in the tumor cell membrane and/or cytoplasm. The quality of immunohistochemical staining was confirmed by comparing tissue sections that were incubated without the primary antibody (negative control). Two pathologists blinded to the clinical and follow-up data independently evaluated the immunostained tissues. The staining index (0–12) was calculated by multiplying the intensity of positive staining (negative, 0; weak, 1; moderate, 2; or strong, 3) and the proportion of immune positive cells of interest (<25%, grade 1; 25–49%, grade 2; 50–74%, grade 3; or >75%, grade 4) [10]. All scores were subdivided into two categories according to a cut-off value of the receiver operating characteristic (ROC) curve in the study cohort: low expression (≤7) and high expression (>7).

Follow-up. The duration of follow-up was calculated from the first day of treatment to either the day of death or the day of the last follow-up. Patients were examined at least every 3 months during the first 2 years, and every 6 months thereafter until death. At every follow-up, the disease status was assessed using a complete physical examination, nasopharyngoscopy, blood and biochemistry profiles, chest radiography, abdominal ultrasonography, and CT/MRI scans of the nasopharynx and cervical region.

Statistical analysis. We used Statistical Package for the Social Sciences version 24.0 (SPSS, Chicago, IL, USA) and R version 3.6.1 (The R Foundation) for statistical analysis. Receiver operating characteristic (ROC) curve analysis was used to obtain cut-off values of WTAP expression. We defined the ideal cut-off point by maximizing the conditional Youden score (i.e., maximum sensitivity and specificity). Spearman's correlation analysis was used to investigate the relationship between tumor-infiltrating immune cells and WTAP expression. We compared and analyzed the clinical characteristics between the WTAP low- and high-expression groups using the chi-square test (or Fisher's exact test, if indicated). All events were measured from the start of treatment. The following endpoints (time to the first defined event) were assessed: overall survival (OS), progression-free survival (PFS), locoregional relapse-free survival (LRRFS), and distant metastasis-free survival (DMFS). Actuarial rates were calculated using the Kaplan-Meier method. Multivariate analyses using the Cox proportional hazards model were used to test for independent significance using backward elimination of insignificant explanatory variables of different parameters. Host factors (age and sex) were included as covariates in all tests. The criterion for statistical significance was set at p=0.05; p-values were determined using two-sided tests.

Results

WTAP overexpression in nasopharyngeal carcinoma. As is shown in Figure 1A, the WTAP was significantly overexpressed in NPC tissue compared to normal tissue in GSE12452. The volcano plot (Figure 1B) showed the differentially expressed genes between tumor and normal tissues. The top 20 most correlated with WTAP in GSE12452 were plotted in the heatmap (Figure 1C). The overexpression of WTAP in GSE12452 was validated by IHC analysis with 100 NPC patients (Figure 1D). In addition, the independent datasets GSE150430 and GSE39826 from the GEO database were applied to validate the expression of WTAP. The GSE150430 generated single-cell transcriptome profiles for 7,581 malignant cells and 666 non-malignant epithelial cells from fifteen primary NPC patients and one normal sample. As is shown in Figure 1E, the WTAP expression in NPC was significantly higher than in non-malignant epithelial cells (p<0.001). In addition, GSE39826 also validated the high expression level of WTAP in NPC cell line and normal epithelial cell line. The

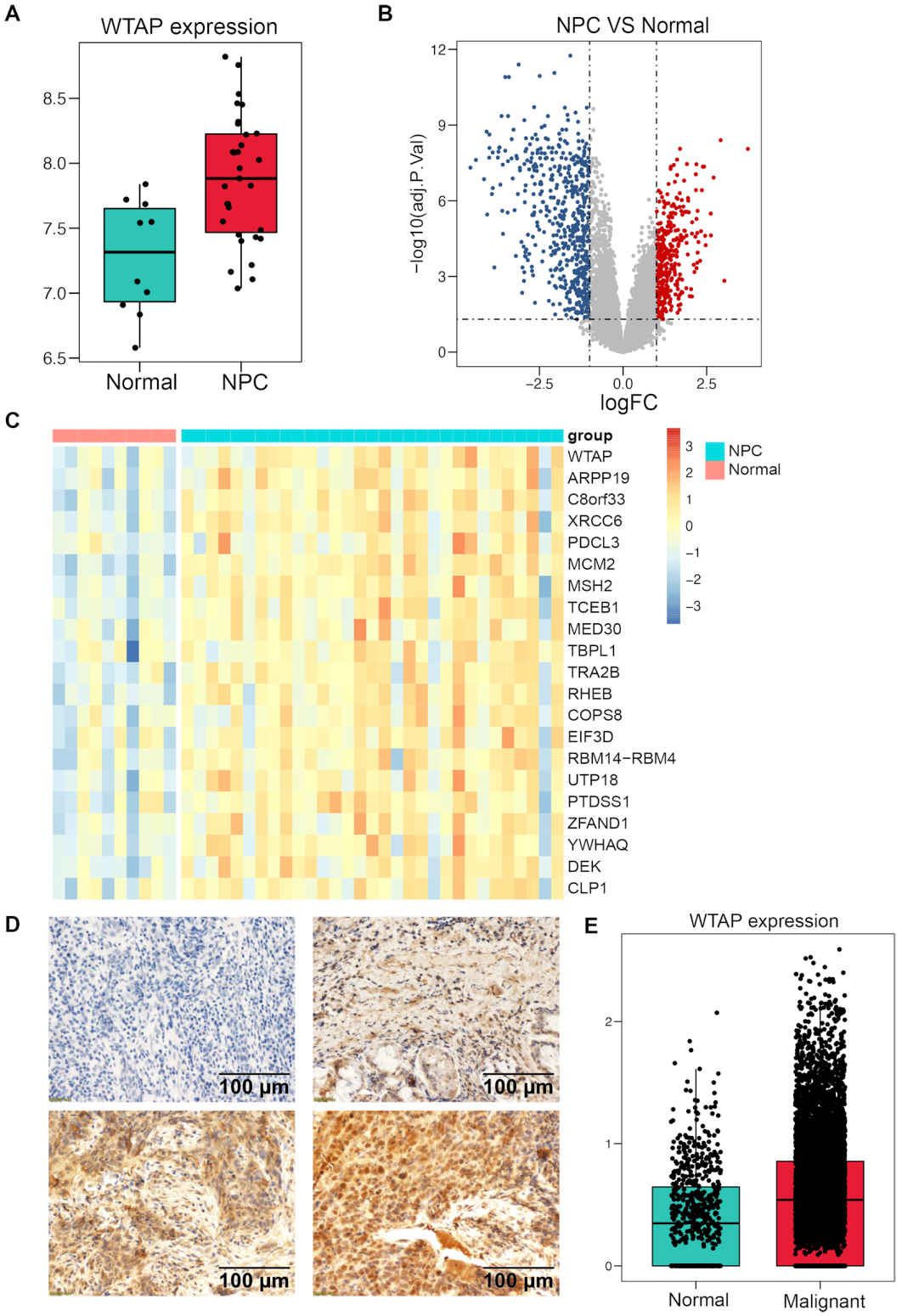

Figure 1. The expression of Wilms' tumor 1-associated protein (WTAP) in nasopharyngeal carcinoma (NPC) tissues and normal tissues revealed by bioinformatics analysis and immunohistochemistry, respectively, of clinical biopsy samples. A) WTAP is upregulated in NPC tissues in GSE12452; B) volcano plot of GSE12452; C) heatmap of top 20 genes most correlated with WTAP in GSE12452; D) representative images of WTAP immunohistochemistry of NPC tissues (Scale bar = 50 μm; original magnification 200×); E) The overexpression of WTAP in NPC tissues is validated in GSE150430 ($p<0.001$).

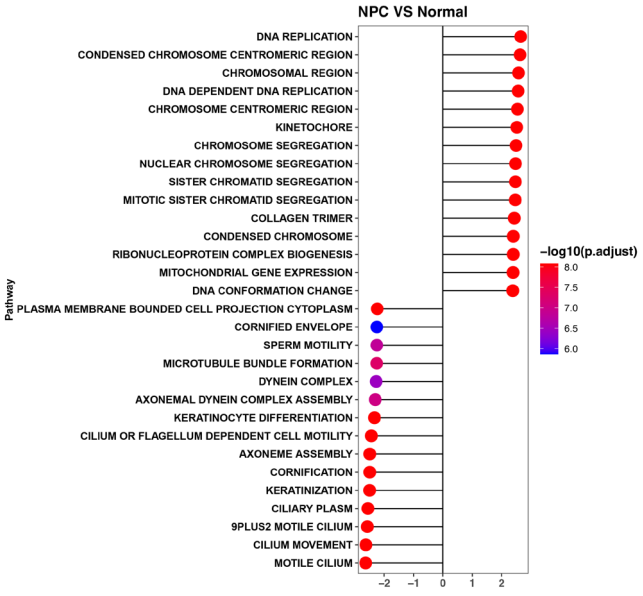

Figure 2. GO enrichment analysis of GSE12452.

expression level of WTAP in C666 (NPC cell line) was significantly high than in primary epithelial cells (log FC 0.4427, p<0.001).

GO enrichment analyses of co-expressed genes of WTAP indicated enrichment in the DNA replication and condensed chromosome centromeric region (Figure 2). Besides, GSEA revealed that DEGs between NPC samples and normal samples were enriched in E2F-targets, Myc_targets_v1, G2M checkpoint, Myc_targets_v2, and Interferon-alpha-response, as is shown in Figure 3A. The GSEA analysis between the WTAP-high cohort and WTAP-low cohort showed that DEGs were enriched in Myc-targets-v1, E2F-targets and G2M checkpoint, MTORC1-signaling, and unfolded-protein-response (Figure 3B).

To further investigate the relationships between WTAP and other genes, correlations were analyzed. As is shown in Table 1, the top 5 genes positively correlated with WTAP in NPC patients (n=31) of GSE12452 were EIF4H, PDCL3, ARPP19, SNHG5, and PEX7.

Correlation of WTAP differential expression with T stage and N stage. Table 2 shows the clinical characteristics of 100 patients with NPC. The study sample included 74 male and 26 female patients, with a median age of 52 years (range 17–79 years). There were 1 (1%), 10 (10%), and 89 (89%) patients diagnosed with type I, type II, and type III disease, respectively, according to the World Health Organization (WHO) criteria. All patients were restaged according to the 8th edition of the UICC/AJCC staging system (N stage). The stage distribution was as follows: stage I, 5 (5%); stage II, 10 (10%); stage III, 43 (43%); stage IVa, 37 (37%); stage IVb, 5 (5%). Forty patients (40%) showed EBV-DNA load

Table 1. Top 20 genes which were correlated with WTAP expression in NPC patients (n=31).

Gene ID	Correlation coefficient	p-value
EIF4H	0.73786915	2.17E-06
PDCL3	0.72513945	3.94E-06
ARPP19	0.70881379	8.09E-06
SNHG5	0.688065	1.89E-05
PEX7	0.68448631	2.17E-05
MMADHC	0.66147379	5.08E-05
HBS1L	0.65969761	5.41E-05
TCEB1	0.65934122	5.48E-05
ZNF706	0.65288371	6.86E-05
ASAP1	0.64904498	7.82E-05
PSMB1	0.64843935	7.98E-05
RHEB	0.64012715	0.000105
VTA1	0.63891175	0.000109
SMIM13	0.63798586	0.000112
RNF11	0.63739646	0.000115
TBPL1	0.6359195	0.000120
44625	0.62988872	0.000146
TYMS	0.62938673	0.000148
GGH	0.62838159	0.000153
AZIN1	0.62498465	0.000170

Table 2. Clinical characteristics of 100 patients with nasopharyngeal carcinoma.

Characteristics	WTAP-low	WTAP-high	p-value
All cases	78	22	
Age (years)			
≤50	33	10	0.792
>50	45	12	
Sex			
Male	60	14	0.21
Female	18	8	
Histology			0.311
WHO I	1	0	
WHO II	6	4	
WHO III	71	18	
T classification*			0.047
T1-3	47	8	
T4	31	14	
N classification*			0.018
N0–1	47	7	
N2–3	31	15	
Chemotherapy			0.583
Yes	73	22	
No	5	0	
EBV-DNA (copy/ml)			0.115
<500	50	10	
≥500	28	12	

Note: *according to the 8th American Joint Commission on Cancer/Union for International Cancer Control staging system; Abbreviation: WHO-World Health Organization

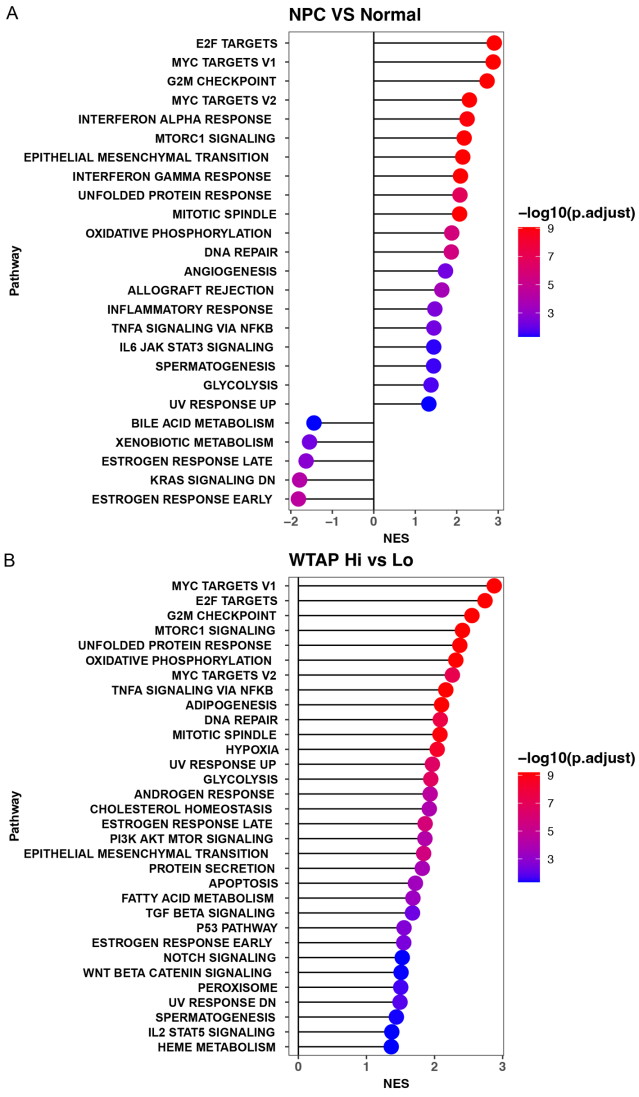

Figure 3. GSEA analysis for NPC samples vs. normal samples (A) and GSEA analysis for the cohort with high-WTAP and low-WTAP expression.

exceeding 500 copies/ml at first diagnosis. The correlation between WTAP immunoexpression and clinicopathological characteristics was assessed by the chi-square test. The results showed that high levels of WTAP expression were significantly correlated with the advanced T stage (p=0.047) and advanced N stage (p=0.018; Table 2).

Correlation of WTAP overexpression with poor prognosis in patients with NPC. The median follow-up time was 47 months (range: 10–63 months). Nine patients (9%) developed locoregional relapse, 23 patients (23%) developed distant metastatic disease, and 3 patients (3%) experienced both locoregional and distant failure. Sixteen patients (16%) died during the follow-up period.

Univariate analyses with log-rank tests showed that the 4-year OS, PFS, LRRFS, and DMFS rates were significantly

Table 3. Summary of multivariate analysis of prognostic factors in 100 patients with nasopharyngeal carcinoma.

Endpoint	HR (95% CI)	p-value
OS		
WTAP expression (low vs high)	4.747 (1.671–13.482)	0.003
T classification (T1–2 vs. T3–4)	5.243 (1.138–24.151)	0.033
N classification (N0–1 vs. N2–3)	5.773 (1.567–20.971)	0.008
PFS		
WTAP expression (low vs. high)	5.171 (1.884–14.193)	0.001
T classification (T1–2 vs. T3–4)	4.531 (1.232–16.665)	0.023
N classification (N0–1 vs. N2–3)	5.773 (1.601–20.536)	0.007
DMFS		
WTAP expression (low vs. high)	2.871 (1.224–6.735)	0.015
T classification (T1–2 vs. T3–4)	3.534 (1.155–10.81)	0.027
N classification (N0–1 vs. N2–3)	7.028 (2.314–21.341)	0.001
LRRFS		
WTAP expression (low vs. high)	6.914 (1.818–26.294)	0.005

Table 4. The mean staining index of IHC biomarkers in cohort with different WTAP expression levels.

Biomarkers	High WTAP	Low WTAP	p-value
CD8a	2.8	5.3	0.001
CD68	4.8	4.7	0.107
CD206	4.5	3.8	0.018
CD200	4.9	4.2	0.588
Foxp3	4.4	4.6	0.759
PD-L1	5.4	5.8	0.439

lower in the WTAP high-expression group (WTAP low- vs. high-expression groups: OS=88.5% vs. 58.7%, p<0.0001; PFS=82.9% vs. 47.1%, p=0.001; LRRFS=94.6% vs. 74.6%, p=0.004; DMFS=84.7% vs. 47.1%, p<0.0001; Figure 4). Multivariate models with Cox proportional hazards analyses confirmed that WTAP was an independent prognostic factor for all the endpoints (OS: hazard ratio [HR], 4.747; 95% confidence interval [CI], 1.671–13.482; p=0.003; PFS: HR [95% CI]=5.171 [1.884–14.193], p=0.001; DMFS: HR [95% CI]=2.871 [1.224–6.735], p=0.015; and LRRFS: HR [95% CI]=6.914 [1.818–26.294], p=0.005; Table 3).

Association of WTAP mRNA expression with immune cells and PD-L1. The interaction between the immune cells and the tumor is an important feature for the prognosis and treatment of cancer. We first examined the relationship between WTAP mRNA expression and immune cell infiltration. We focused on the immune markers of T cells (Figure 5A), Treg cells (Figure 5B), B cells (Figure 5C), M1 cells (Figure 5D), Th2 cells (Figure 5E), M2 cells (Figure 5F), and Th1 cells (Figure 5G) and PD-1/L1 (Figure 5H) in GSE12452. The results showed that WTAP expression was positively correlated with CD200 (r=0.549; p<0.001), MRC1 (r=0.408; p=0.008), STAT1 (r=0.446; p=0.003), CCR8 (r=0.339; p=0.003), PD-1 (r=0.32; p=0.04) expres-

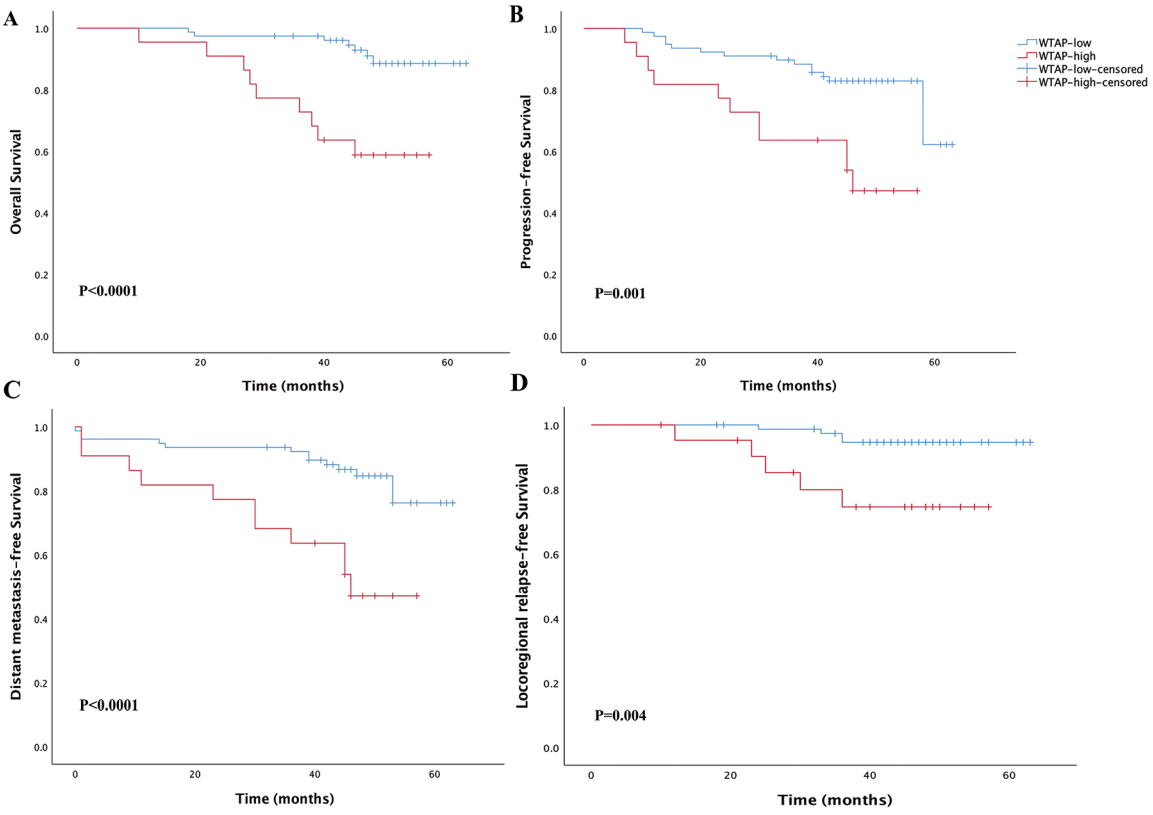

Figure 4. The Kaplan-Meier estimated survival curves for 100 patients with nasopharyngeal carcinoma (NPC) stratified by WTAP expression levels. A) overall survival (OS); B) progression-free survival (PFS); C) distant metastasis-free survival (DMFS); D) locoregional relapse-free survival (LRRFS). P values were calculated with the unadjusted log-rank test.

sion and negatively correlated with IL13 (r=–0.33; p=0.035), STAT6 (r=–0.305; p=0.05), and FOXP3 (r=–0.395; p=0.011) expression.

Considering that the mRNA expression data lacks spatial information, IHC could characterize the density and spatial distribution of specific immune cells in the tumor immune microenvironment. The correlation of WTAP and biomarkers of immune cells was further confirmed with IHC. As is shown in Table 4, the stain index of CD8a in the WTAP high-expression cohort was significantly lower than in the WTAP low-expression cohort. The series of IHC images of an NPC patient with high WTAP expression staining is shown in Figure 6. On the contrary, the stain index of CD206 and PD-L1 was significantly higher in the WTAP high-expression cohort. The stain indexes of CD163, CD200, and FOXP3 were similar between the WTAP high-expression cohort and the low-expression cohort.

Discussion

Understanding the molecular mechanism of tumor occurrence and development is the basis of precision therapy. Several novel biomarkers have been identified to be key genes for the development of NPC, which facilitates prognostic risk stratification and molecular targeted therapy development. At present, there are few studies on m6A methylation in NPC. In the present study, we found that WTAP was overexpressed in NPC and high levels of WTAP expression were a biomarker of poor prognosis in patients with nasopharyngeal carcinoma. These results may provide a foundation for further exploring the biological significance of m6A methylation in NPC.

m6A-mediated RNA methylation is an important epitranscriptomic modification that modulates gene expression in NPC. Zhang et al. were the first to investigate the m6A-mediated low expression level of ZNF750 (encoding zinc finger protein 750), which modulates NPC progression via the ZNF750-FGF14 signaling axis [21]. Expression of the m6A methyltransferase METTL3 in NPC was also investigated; the results showed that METTL3 was remarkably highly expressed in NPC tissues and cell lines. Patients with METTL3 high expression exhibited poor prognosis. Molecular biology experiments showed that METTL3 binds to EZH2 mRNA and inhibits EZH2 expression by mediating m6A modification, which further modulates the expression of CDKN1C and promotes the progression of NPC

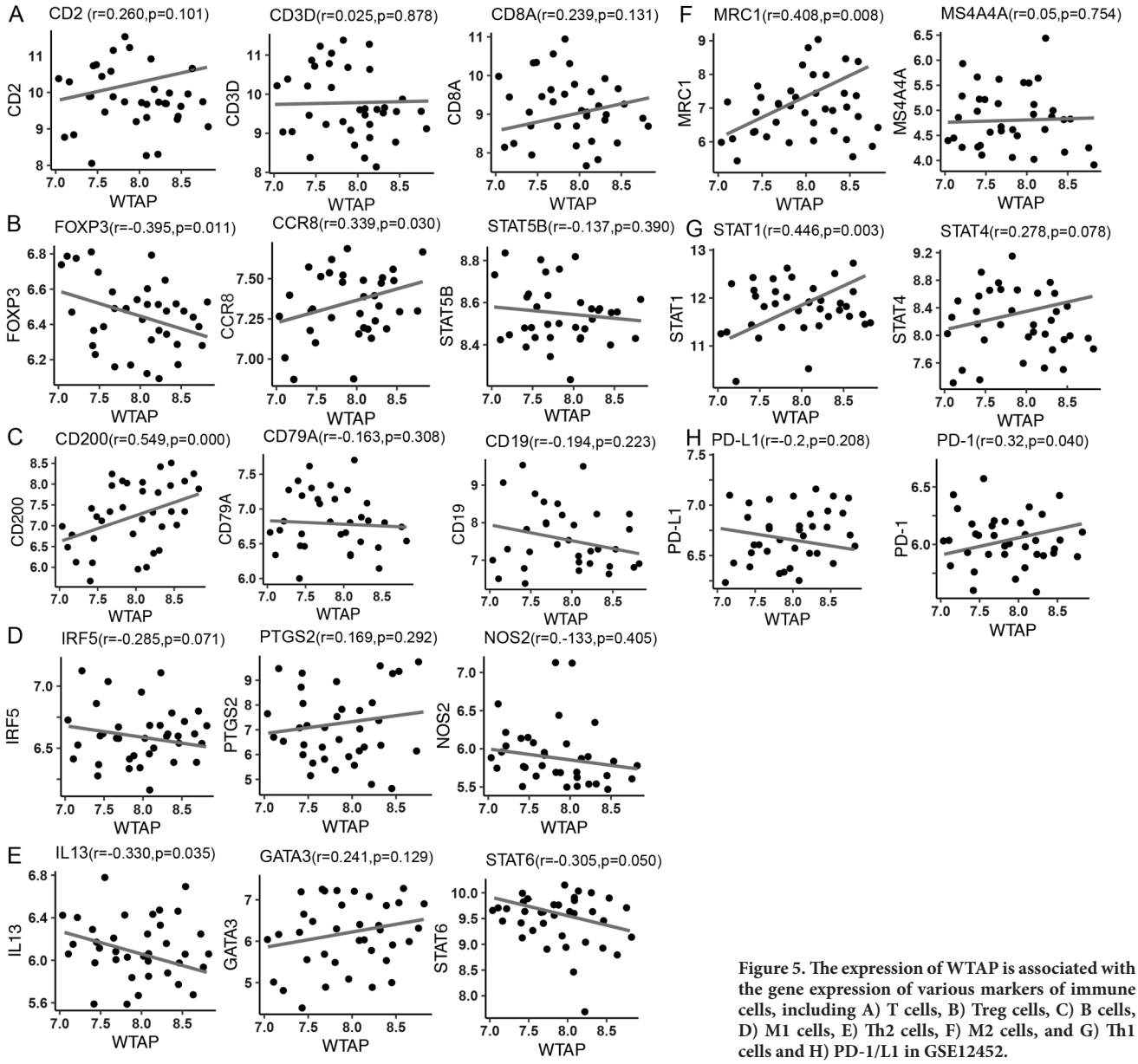

Figure 5. The expression of WTAP is associated with the gene expression of various markers of immune cells, including A) T cells, B) Treg cells, C) B cells, D) M1 cells, E) Th2 cells, F) M2 cells, and G) Th1 cells and H) PD-1/L1 in GSE12452.

[22]. Furthermore, Lu et al. analyzed the expression and prognostic value of m6A-related genes using the GSE68799, GSE53819, and GSE103611 datasets of the GEO database. The authors established a prognostic risk model based on three m6A-related genes (GF2BP1+IGF2BP2+METTL3), which is an independent prognostic factor in NPC [23].

WTAP is a component of the m6A methyltransferase complex; it recruits the m6A methyltransferases METTL3 and METTL14 to the corresponding mRNA targets to participate in the formation of m6A. WTAP expression is negatively correlated with the malignant progression of various cancers but has never been studied in NPC. In the present study, we found that WTAP was upregulated in NPC, and the high expression levels of WTAP were correlated with the advanced T stage and the advanced N stage. A previous study revealed that WTAP could promote metastasis by stabilizing Fak mRNA in pancreatic cancer [24]. In this study, the fact that the expression level of WTAP in patients with lymph node metastasis was significantly higher than those without lymph node metastasis also confirmed this. Gene ontology enrichment analysis of genes co-expressed with WTAP also indicated that WTAP is involved in cell cycle regulation; a dysregulated cell cycle is a hallmark of carcinogenesis. Consistent with these findings, a previous study by Chen et al. showed that WTAP knockdown caused G2/M arrest; p21/p27 upregulation; and CDC25C, CDK1, cyclin-A2, and

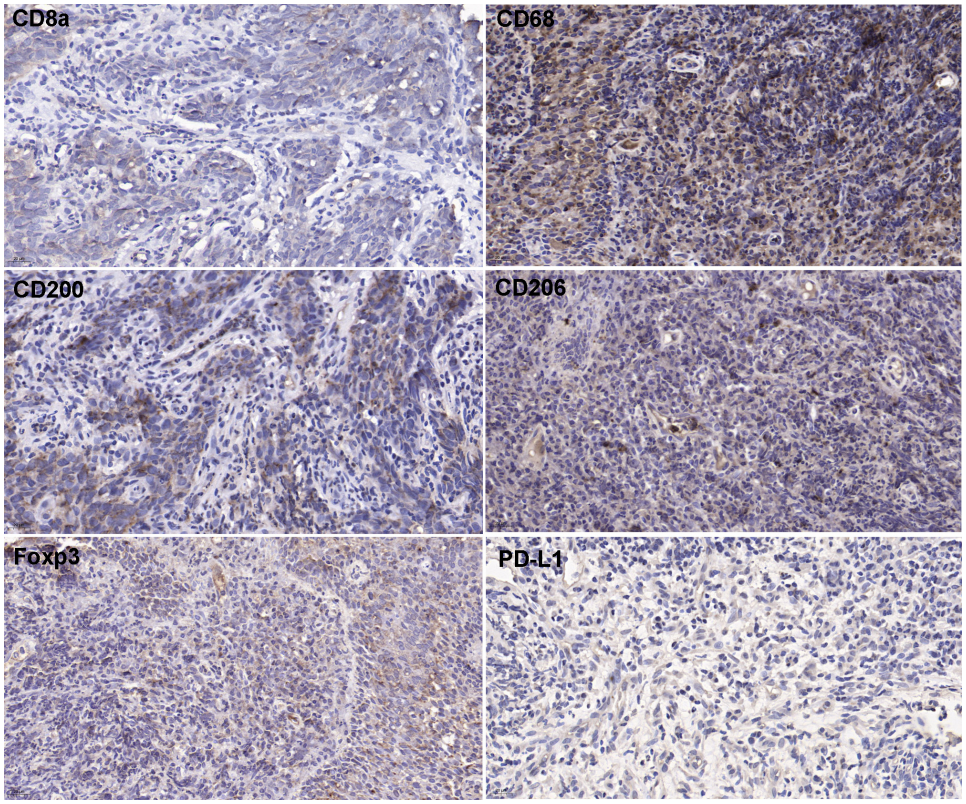

Figure 6. Representative IHC image of an NPC patient with high WTAP expression staining. The IHC biomarkers including CD8a, CD68, CD200, CD206, Foxp3, and PD-L1. Original magnification, 40×.

cyclin-B1 downregulation; in contrast, WTAP overexpression reduced the expression of p21 and p27 and all the indicated checkpoint proteins in the G2 phase in hepatocellular carcinoma. They further discovered that WTAP-mediated m6A methylation led to post-transcriptional suppression of ETS proto-oncogene 1 (ETS1), which mediated G2/M arrest in a p21/p27-dependent manner [25]. In the GSEA analysis, the Myc-targets-v1 was enriched both in the GSEA analysis of NPC samples vs. normal samples and WTAP-high cohort and WTAP-low cohort. The MYC oncogenes encode a family of transcription factors, which were among the most commonly activated oncoproteins in human malignancies [26]. In addition, the top 5 genes positively correlated with WTAP were EIF4H, PDCL3, ARPP19, SNHG5, and PEX7. Previous studies revealed that EIF4H and Arpp19 could promote Myc expression and increase cell migration in malignancy [27, 28]. On the other hand, MYC was reported to upregulate the expression of immune-checkpoint proteins, such as PD-L1 and CD47, thus leading to $CD8^+$ T cell exhaustion [29]. Besides, MYC could also promote the expression of several cytokines (CCL2, IL-23, and CCL9, etc.). These cytokines could promote the conversion of anti-tumor M1 macrophages to pro-tumor M2 macrophages and prevent the activation and recruitment of B cells, NK cells, and $CD8^+$ T cells [30]. The polarization of immunosuppressive macrophages facilitated the progression of cancer. The IHC results in this study confirmed the more M2 macrophages and lower $CD8^+$ T cells in patients with high WTAP expression. Based on the above results, we assumed the WTAP might facilitate immune escape in NPC patients by regulating the expression of MYC through EIF4H and Arpp19. But the detailed mechanisms of how WTAP-related immune infiltration put a hazardous effect on NPC remain to be confirmed.

Immune cell infiltration in NPC is closely associated with patient prognosis. Lu et al. analyzed the prognostic value of inflammatory cell density in NPC. The results showed that patients with a low density of tumor-infiltrating $FOXP3^+$ $CD8^+$ T-lymphocytes, neutrophils, and mast cells and a high density of NK cells showed a significantly better outcome. However, PD-1 positivity predicted poor prognosis in patients with NPC [31]. In the present study, WTAP expression was positively correlated with CD200, MRC1, and STAT1 expression. Recent studies discovered that CD200-CD200 receptor (CD200R) interaction plays a vital role in regulating the tumor microenvironment and tumor development [32, 33]. CD200 is overexpressed in neuroblastoma and decreases anti-tumor immunity in the tumor microenvironment. A lower number of $CD4^+$ $CD8^+$ T cells and lower IFN-γ and/or TNF-α expression were observed in neuroblastoma tumors with higher CD200 expression [33]. MRC1 is a marker of M2-like tumor-

associated macrophages that contribute to tumor immunosuppression, relapse, and metastasis in various solid tumors [34]. STAT1 prompts immunosuppression by enhancing the infiltration of myeloid-derived suppressor cells [35]. In this study, WTAP expression was negatively correlated with CD8a expression but positively correlated with CD206 (M2 macrophages marker). The results indicated that the influence on prognosis led by WTAP could potentially result from WTAP-dependent immune cell infiltration level. Together, these findings suggest that WTAP may promote the tumorigenesis and progression of NPC by regulating immune cell infiltration.

In the present study, we found that patients with high WTAP expression were more likely to develop local recurrence and distant metastasis, indicating that these patients might benefit from more aggressive therapy such as molecular targeted therapy or immunotherapy. Although we preliminarily explored the biological function of WTAP in NPC using gene ontology enrichment analysis, further biomedical experiments are required to understand the mechanism in depth. Nevertheless, the present findings are encouraging and provide new insight into the identification of promising prognostic biomarkers and therapeutic targets for NPC.

In conclusion, WTAP is upregulated in NPC, and high levels of WTAP expression were a biomarker of poor prognosis in patients with NPC. Moreover, WTAP expression was correlated with the expression of immune cell biomarkers such as CD206 and CD8a, which are key molecules that regulate the tumor microenvironment. WTAP may serve as a promising prognostic biomarker and therapeutic target for NPC.

Acknowledgments: This work was supported by grants from the Medical Health Science and Technology Project of the Zhejiang Provincial Health Commission (No. 2020RC044).

References

[1] BRAY F, FERLAY J, SOERJOMATTARAM I, SIEGEL RL, TORRE LA et al. Global cancer statistics 2018: GLOBOCAN estimates of incidence and mortality worldwide for 36 cancers in 185 countries. CA Cancer J Clin 2018; 68: 394–424. https://doi.org/10.3322/caac.21492

[2] JIANG F, JIN T, FENG XL, JIN QF, CHEN XZ. Long-term outcomes and failure patterns of patients with nasopharyngeal carcinoma staged by magnetic resonance imaging in intensity-modulated radiotherapy era: The Zhejiang Cancer Hospital's experience. J Cancer Res Ther 2015; 11: C179–C184. https://doi.org/10.4103/0973-1482.168181

[3] ZHANG LL, HUANG MY, FEI X, KE XW, DI S et al. Risk stratification for nasopharyngeal carcinoma: a real-world study based on locoregional extension patterns and Epstein-Barr virus DNA load. Ther Adv Med Oncol 2020; 12: 1758835920932052. https://doi.org/10.1177/1758835920932052

[4] LIANG Y, LI J, LI Q, TANG LL, CHEN L et al. Plasma protein-based signature predicts distant metastasis and induction chemotherapy benefit in Nasopharyngeal Carcinoma. Theranostics 2020; 10: 9767–9778. https://doi.org/10.7150/thno.47882

[5] WANG T, WU J, WUY, CHEN Y, DENG Y et al. A novel microRNA-based signature predicts prognosis among nasopharyngeal cancer patients. Exp Biol Med (Maywood) 2021; 246: 72–83. https://doi.org/10.1177/1535370220958680

[6] WANG YQ, CHEN L, MAO YP, LI YQ, JIANG W et al. Prognostic value of immune score in nasopharyngeal carcinoma using digital pathology. J Immunother Cancer 2020; 8: e000334. https://doi.org/10.1136/jitc-2019-000334

[7] ZHONG LZ, FANG XL, DONG D, PENG H, FANG MJ et al. A deep learning MR-based radiomic nomogram may predict survival for nasopharyngeal carcinoma patients with stage T3N1M0. Radiother Oncol 2020; 151: 1–9. https://doi.org/10.1016/j.radonc.2020.06.050

[8] SUN T, WU R, MING L. The role of m6A RNA methylation in cancer. Biomed Pharmacother 2019; 112: 108613. https://doi.org/10.1016/j.biopha.2019.108613

[9] LITTLE NA, HASTIE ND, DAVIES RC. Identification of WTAP, a novel Wilms' tumour 1-associating protein. Hum Mol Genet 2000; 9: 2231–2239. https://doi.org/10.1093/oxfordjournals.hmg.a018914

[10] LI BQ, HUANG S, SHAO QQ, SUN J, ZHOU L et al. WT1-associated protein is a novel prognostic factor in pancreatic ductal adenocarcinoma. Oncol Lett 2017; 13: 2531–2538. https://doi.org/10.3892/ol.2017.5784

[11] CHEN L, WANG X. Relationship between the genetic expression of WTAP and bladder cancer and patient prognosis. Oncol Lett 2018; 16: 6966–6970. https://doi.org/10.3892/ol.2018.9554

[12] LI H, SU Q, LI B, LAN L, WANG C et al. High expression of WTAP leads to poor prognosis of gastric cancer by influencing tumour-associated T lymphocyte infiltration. J Cell Mol Med 2020; 24: 4452–4465. https://doi.org/10.1111/jcmm.15104

[13] NAREN D, YAN T, GONG Y, HUANG J, ZHANG D et al. High Wilms' tumor 1 associating protein expression predicts poor prognosis in acute myeloid leukemia and regulates m(6)A methylation of MYC mRNA. J Cancer Res Clin Oncol 2020; 147: 33–47. https://doi.org/10.1007/s00432-020-03373-w

[14] JIN DI, LEE SW, HAN ME, KIM HJ, SEO SA et al. Expression and roles of Wilms' tumor 1-associating protein in glioblastoma. Cancer Sci 2012; 103: 2102–2109. https://doi.org/10.1111/cas.12022

[15] LI ZX, ZHENG ZQ, YANG PY, LIN L, ZHOU GQ et al. WTAP-mediated m 6 A modification of lncRNA DIAPH1-AS1 enhances its stability to facilitate nasopharyngeal carcinoma growth and metastasis. Cell Death Differ 2022; 29: 1137–1151. https://doi.org/10.1038/s41418-021-00905-w

[16] CHEN YP, YIN JH, LI WF, LI HJ, CHEN DP et al. Single-cell transcriptomics reveals regulators underlying immune cell diversity and immune subtypes associated with prognosis in nasopharyngeal carcinoma. Cell Res 2020; 30: 1024–1042. https://doi.org/10.1038/s41422-020-0374-x

[17] PORT RJ, PINHEIRO-MAIA S, HU C, ARRAND JR, WEI WB et al. Epstein-Barr virus induction of the Hedgehog signalling pathway imposes a stem cell phenotype on human epithelial cells. J Pathol 2013; 231: 367–377. https://doi.org/10.1002/path.4245

[18] LIBERZON A, BIRGER C, THORVALDSDOTTIR H, GHANDI M, MESIROV JP et al. The Molecular Signatures Database Hallmark Gene Set Collection. Cell Systems 2015; 1: 417–425. https://doi.org/10.1016/j.cels.2015.12.004

[19] LEE AW, NG WT, PAN JJ, POH SS, AHN YC et al. International guideline for the delineation of the clinical target volumes (CTV) for nasopharyngeal carcinoma. Radiother Oncol 2018; 126: 25–36. https://doi.org/10.1016/j.radonc.2017.10.032

[20] PANCIONE M, GIORDANO G, REMO A, FEBBRARO A, SABATINO L et al. Immune escape mechanisms in colorectal cancer pathogenesis and liver metastasis. J Immunol Res 2014; 2014: 686879. https://doi.org/10.1155/2014/686879

[21] ZHANG P, HE Q, LEI Y, LI Y, WEN X et al. m(6)A-mediated ZNF750 repression facilitates nasopharyngeal carcinoma progression. Cell Death Dis 2018; 9: 1169. https://doi.org/10.1038/s41419-018-1224-3

[22] MENG QZ, CONG CH, LI XJ, ZHU F, ZHAO X et al. METTL3 Promoes the progressing of nasophryngral carcinoma through mediaitng M6A modification of EZH2. Eur Rev Med Pharmacol Sci 2020; 24: 4328–4336. https://doi.org/10.26355/eurrev_202004_21014

[23] LU S, YU Z, XIAO Z, ZHANG Y. Gene Signatures and Prognostic Values of m(6)A Genes in Nasopharyngeal Carcinoma. Front Oncol 2020; 10: 875. https://doi.org/10.3389/fonc.2020.00875

[24] LI BQ, LIANG ZY, SEERY S, LIU QF, YOU L et al. WT1 associated protein promotes metastasis and chemo-resistance to gemcitabine by stabilizing Fak mRNA in pancreatic cancer. Cancer Lett 2019; 451: 48–57. https://doi.org/10.1016/j.canlet.2019.02.043

[25] CHEN Y, PENG C,CHEN J, CHEN D,YANG B et al. WTAP facilitates progression of hepatocellular carcinoma via m6A-HuR-dependent epigenetic silencing of ETS1. Mol Cancer 2019; 18: 127. https://doi.org/10.1186/s12943-019-1053-8

[26] DHANASEKARAN R, DEUTZMANN A, MAHAUAD-FERNANDEZ WD, HANSEN AS, GOUW AM et al. The MYC oncogene – the grand orchestrator of cancer growth and immune evasion. Nat Rev Clin Oncol 2022; 19: 23–36. https://doi.org/10.1038/s41571-021-00549-2

[27] MAKELA E, LOYTTYNIEMI E, SALMENNIEMI U, KAUKO O, VARILA T et al. Arpp19 Promotes Myc and Cip2a Expression and Associates with Patient Relapse in Acute Myeloid Leukemia. Cancers (Basel) 2019; 11: 1774. https://doi.org/10.3390/cancers11111774

[28] VAYSSE C, PHILIPPE C, MARTINEAU Y, QUELEN C, HIEBLOT C et al. Key contribution of eIF4H-mediated translational control in tumor promotion. Oncotarget 2015; 6: 39924–39940. https://doi.org/10.18632/oncotarget.5442

[29] MAEDA T, HIRAKI M, JIN C, RAJABI H, TAGDE A et al. MUC1-C Induces PD-L1 and Immune Evasion in Triple-Negative Breast Cancer. Cancer Res 2018; 78: 205–215. https://doi.org/10.1158/0008-5472.CAN-17-1636

[30] DHANASEKARAN R, BAYLOT V, KIM M, KURUVILLA S, BELLOVIN D et al. MYC and Twist1 cooperate to drive metastasis by eliciting crosstalk between cancer and innate immunity. Elife 2020; 9: e50731. https://doi.org/10.7554/eLife.50731

[31] LU J, CHEN XM, HUANG HR, ZHAO FP, WANG F et al. Detailed analysis of inflammatory cell infiltration and the prognostic impact on nasopharyngeal carcinoma. Head Neck 2018; 40: 1245–1253. https://doi.org/10.1002/hed.25104

[32] LIU JQ, HU A, ZHU J, YU J, TALEBIAN F et al. CD200-CD200R Pathway in the Regulation of Tumor Immune Microenvironment and Immunotherapy. Adv Exp Med Biol 2020; 1223: 155–165. https://doi.org/10.1007/978-3-030-35582-1_8

[33] XIN C, ZHU J, GU S, YIN M, MA J et al. CD200 is overexpressed in neuroblastoma and regulates tumor immune microenvironment. Cancer Immunol Immunother 2020; 69: 2333–2343. https://doi.org/10.1007/s00262-020-02589-6

[34] CHEN Y, SONG Y, DU W, GONG L, CHANG H et al. Tumor-associated macrophages: an accomplice in solid tumor progression. J Biomed Sci 2019; 26: 78. https://doi.org/10.1186/s12929-019-0568-z

[35] MEISSL K, MACHO-MASCHLER S, MULLER M, STROBL B. The good and the bad faces of STAT1 in solid tumours. Cytokine 2017; 89: 12–20. https://doi.org/10.1016/j.cyto.2015.11.011